Nuclear Science and Techniques **22** (2011) 205–211

Multi-technique characterizations of main elements in the vehicle exhaust particles collected in a tunnel in Shnaghai

JIN Chan[1,2,*] FAN Xiaoyan[1] LI Yan[2] LIANG Feng[2] LI Yulan[2] ZOU Yang[2]
YANG Yongji[1] XIE Yaning[3]

[1]*Department of Biophysics*, *College of Basic Medical Sciences*, *Second Military Medical University*, *Shanghai 200433*, *China*

[2]*Shanghai Institute of Applied Physics*, *Chinese Academy of Sciences*, *Shanghai 201800*, *China*

[3]*Institute of High Energy Physics*, *the Chinese Academy of Sciences*, *Beijing 100039*, *China*

Abstract In this study, vehicle exhaust particles were collected three locations (the middle, entrance and outside) of the Dapu Road tunnel in downtown Shanghai, and the particle samples were characterized using SEM, XAFS, ICP-MS and Mössbauer spectrometry, and the oxidative damage was assessed by plasmid DNA. Most iron-containing particles are found from vehicle exhaust, and iron oxide is the major species in all samples. Its concentration in the particles inside the tunnel is higher than that the outside particles. The iron particles inside the tunnel have higher proportion of water-soluble fraction in hydrous iron sulfate form or smaller size. $ZnCl_2$ is the main soluble fraction in zinc-containing particles, while higher percentage of insoluble fraction existed in the particles outside of tunnel. Major species of lead-containing particles are $PbSO_4$, $Pb_3(PO_4)_2$ and $PbCO_3$. In addition, the soluble fraction of other transition metallic elements as Ti and V is higher in the particles inside the tunnel than that outside the tunnel. The plasmid DNA assay results indicate that the particles from vehicle exhaust have a stronger oxidative damage and inflammation than that from outside of the tunnel.

Key words Vehicle exhaust particles, Main elements, XAFS, ICP-MS, Mössbauer spectrum, Plasmid DNA assay

1 Introduction

During the past decades, physical and chemical properties of nano-sized materials have been studied extensively[1–5]. Several epidemiological studies have found high association of ambient ultrafine particles (<100 nm) with cardiovascular diseases[6–10]. A great amount of nano-sized ambient particles are produced by coal combustion, vehicle exhaust, nano-technological industries etc. They have larger surface area per unit mass, higher number concentration and longer persistence time in atmosphere, and are capable of penetrating cellular targets and reaching the lung[11–13], or even getting into the bloodstream[14]. For understanding toxicity of the particles, it is crucial to clarify their chemical structures.

Synchrotron-based X-ray absorption fine structure (XAFS) is a powerful tool to address this issue. Being a non-destructive technique of parts-per-million (ppm) sensitivity for many elements, it is widely used to characterize chemical complexity of the elements contained in small size particles, providing rich information about their molecular structure and speciation[15–17].

Vehicle exhaust particles are major air pollution causing health and environment problems in large cities in China. There are about 3 million motor vehicles in Shanghai, and this number increases rapidly. A tunnel is a typical location where vehicle exhaust emissions are high, especially in the center of tunnels. Our previous work showed that α-Fe_2O_3 ultrafine particles of about 13 nm were main species of iron-containing particles produced by vehicle exhaust [15]. In this work, XAFS, inductively coupled plasma-

---

.JIN Chan and FAN Xiaoyan contributed eqully to this work

* Corresponding author. *E-mail address*: jinchan2010@yahoo.cn

Received date: 2011-03-30

mass spectrometry (ICP-MS) and Mössbauer spectrometry (MS) were used to study molecular structure of the vehicle exhaust particles collected in the middle part of Dapu Road tunnel, the oldest tunnel in Shanghai. Particles outside the tunnel were collected as the control. Toxicity of the water-soluble fraction was studied by using plasmid DNA.

2 Experimental

2.1 Sample collection

The aerosol samples were taken for 14 days in February 2005 with a cascade impact air sampler ($PM_{10-2.5}$, Beijing Geological Instrument Factory) at Dapu Road tunnel, a two-lane tunnel of about 3 km. The samples were collected at three positions of the tunnel, the middle part (about 1.5 km to the entrance), the outside (~0.2 km to the entrance), and the entrance. The sampling height was 1.5 m above the ground at a flow rate of 78 L/min. The particles were trapped onto a Φ90 mm Cellulose filter (Millipore Company).

2.2 XAFS measurement

The XAFS spectra were obtained on BL-12C experimental station of the Photon Factory, High Energy Accelerator Research Organization (KEK) in Tsukuba, Japan and 4W1 experimental station of Beijing Synchrotron Radiation Facility (BSRF), China. Higher harmonics were reduced sufficiently by detuning the double-crystal Si(111) monochromator at BL-12C and 4W1. The XAFS experiments were conducted in fluorescence detection mode using either a Lytle (4W1) or a 19-element Ge array detector (BL-12C) [16,17], depending on concentration of the metal elements in the samples. The reference samples were measured in transmission mode. Energy calibration was performed using a foil of either a metal or oxide of an appropriate element. The zinc K-edge and lead L(III)-edge XAFS spectra were collected. The raw data was analyzed using the IFEFFIT program[18,19] according to standard data analysis procedures[20].

2.3 ICP-MS measurement

The particles scraped from the filters were digested in a microwave oven (Milestone Ethos), followed by 5 times ultrasonic to obtain the water-soluble fraction. Each vessel was added with 4 mL of 65% HNO_3 and 1 mL of 30% H_2O_2 (Jing Rui Chen. Co.). The digest was transferred into a beaker and diluted with pure water to a final volume of 25 mL. The concentrations of Ti, V, Zn and Pb were analyzed by ICP-MS (Thermo Elemental X7) in standard mode. ^{115}In was used as the internal standard. The determination of iron concentration was performed by collision/reaction cell technology (CCT) mode of the ICP-MS. Accuracy of the analysis was validated by NIST reference material 1648 (urban particulate matter).

2.4 Mössbauer spectrometry

The iron species was checked by Mössbauer spectrometry in transmission geometry with a constant acceleration. A ^{57}Co(Pd) Mössbauer source was used. A 1-mm thick Na(TI) scintillator was coupled to EMI9750B photoelectric multiplier. At room temperature, 80 K and 15 K, each sample was measured for 10 days to achieve ~1.5×10^6 counts per channel. The fraction of intensity contributed by non-Mössbauer line was derived from the energy spectrum. The isomer shift values reported in this work were relative to α-Fe at room temperature. Mössbauer data were fitted by a least-squares fitting program.

2.5 The plasmid DNA assay

The plasmid DNA assay developed by Greenwell[21,22] was used. Soluble fraction of the particles at different concentrations and pure water were incubated. All incubations were carried out to final volume of 18 μL, which contained 1 μL plasmid DNA in the concentration of 1 μg/μL pBR322 purchased from Shanghai Sino-American Biotechnology Co. Ltd. Incubation were gently agitated to ensure the maximum mixing of the sample and avoid sedimentation for 6 h at room temperature. In addition, bromophenol blu/glycerol-loading dye (2 μL) was added to each sample before assaying. The gels comprised of 0.9% agarose and 0.5% ethidium bromide was run in 80-eV electrophoretic current for 5 h at room temperature in 1% Tris-Borate-EDTA (TEB) buffer. The Syngene Genesnap code (Synoptics Ltd., Cambridge, UK) was used to image gels and quantify different forms of DNA. The toxic dose causing 20% damage to DNA, was calculated by a linear regression.

3 Results and Discussion

Morphology of the particles was examined by scanning electron microscopy (SEM, LEO-1530VP). The particles collected in middle part of the tunnel (Fig.1a) are spherical and small, while the particles collected outside the tunnel (Fig.1b) are of large-size irregular shape.

Concentration of the main metal elements in the particles, and the water-soluble fraction, determined by ICP-MS, are given in Table 1.

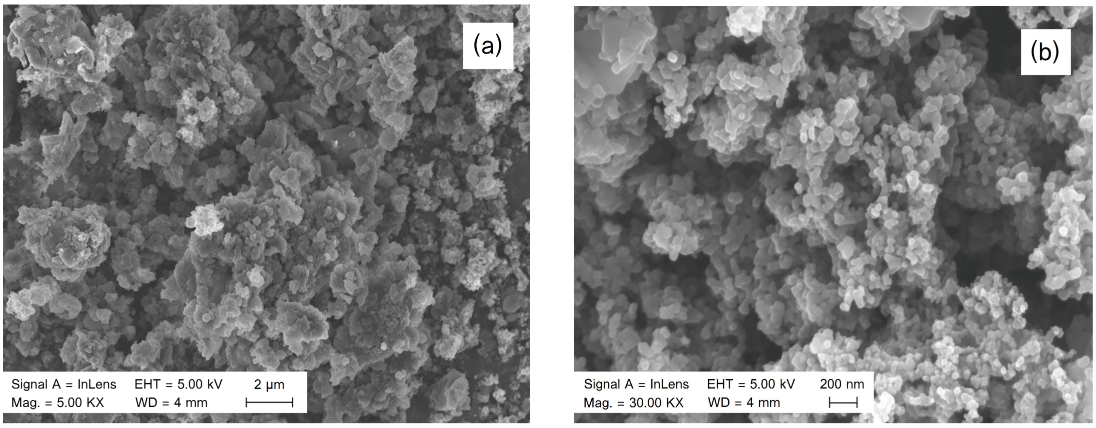

Fig.1 SEM images of particles collected outside the tunnel (a) and in middle part of the tunnel (b).

Table 1 Concentration (in µg/g) of main metals in particles collected at different parts of the Dapu tunnel.

Elements	Micro-sized particles (the outside)		Mixed particles (entrance)	Nano-sized particles (the middle)	
	Total	Water-soluble	Total	Total	Water-soluble
Ti	624.8±12.4	1.4±0.07	729.7±8.4	819.5±20.7	7.3±0.4
V	103.0±1.3	2.9±0.1	84.2±1.5	67.3±0.7	27.4±1.1
Fe	30100.0±300.0	298.9±6.1	32300.0±100.0	40500.0±100	408.0±25.8
Zn	9700.0±100.0	1042.0±7.3	2800.0±200.0	17000.0±1.0	2017.0±45.6
Pb	939.4±20.6	27.0±0.4	443.5±15.1	308.1±1.8	33.8±0.2

The iron concentration decreased from the middle part to the outside. The particles outside the tunnel have a small water-soluble fraction, which suggests that the iron particles may be originated mainly from the vehicle exhaust, produced possibly in reactions between steel engine cylinders and oxygen or NO_x at high temperature. Sioutas *et al.* [22]found that atmospheric ultrafine particles (UFP) in sizes of less than about 0.1 µm were formed by a variety of gas-to-particles conversion processes at high temperature.

While the fraction of water soluble iron-containing particles collected inside the tunnel is higher than that the outside, the lead concentration of the particles outside the tunnel is three times higher than that inside the tunnel, indicating that vehicle exhaust is no longer a major contribution to atmosphere in Shanghai after phasing-out of leaded gasoline in 1997. But the soluble fraction of lead in ultrafine particles collected outside and inside the tunnel is 27.0±0.4 ppm and 33.8±0.2 ppm, respectively, with only a tiny fraction of lead-containing particles dissolved.

The zinc content in particles outside of the tunnel is five times higher than the inside, but the water-soluble fraction in the particles outside the tunnel (1042.0±7.3 ppm) is about half of the particles inside the tunnel (2017.0±45.6 ppm), indicating that zinc is easier to accumulate in small- sized particles than dispersed in the water. The V and Ti concentrations in particles outside the tunnel are a litter higher than inside, but their concentrations in water-soluble fraction for the particle inside the tunnel is higher than that the outside.

Generally, the water-soluble fractions of the five metal elements in particles inside the tunnel are much higher than the outside, suggesting that toxicity of particles inside the tunnel may be stronger than the particles outside the tunnel.

The Mössbauer spectra are measured at room temperature and 15 K with ultrafine particles collected at different tunnel sites, as shown in Fig.2. The fitted results are given in Table 2.

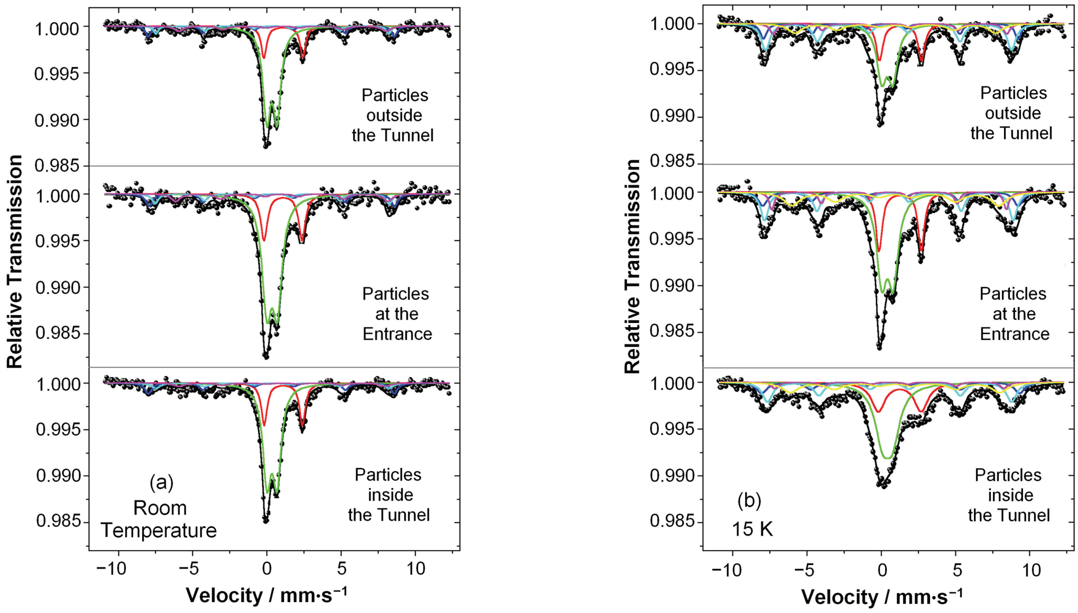

Fig.2 Mössbauer spectra of the particles collected at the tunnel sites, measured at room temperature and 15 K.

Table 2 IS(mm/s), QS (mm/s), A(%) and Heff (T) of Mössbauer spectra measured at room temperature and 15 K with particles of micro-, mixed- and nano-sizes collected at the tunnel outside, entrance and middle, respectively.

Spectral		Room temperature			15 K		
Parameters		Outside	Eentrance	Middlel	Outside	Entrance	Middle
Doublet	IS	1.12(2)	1.01(2)	1.12(2)	1.30(2)	1.28(1)	1.25(2)
component (A)	QS	2.62(2)	2.56(1)	2.57(2)	2.83(2)	2.84(2)	2.88(1)
	A	18(2)	18(2)	15(2)	14(2)	15(1)	18(2)
Doublet	IS	0.35(2)	0.37(2)	0.36(1)	0.42(2)	0.43(2)	0.42(2)
component (B)	QS	0.69(1)	0.71(2)	0.68(2)	0.67(1)	0.77(2)	0.75(1)
	A	58(2)	59(2)	59(2)	29(2)	33(2)	35(2)
Sextet	IS	0.40(2)	0.40(2)	0.40(2)	0.43(2)	0.41(2)	0.48(2)
component (A)	Heff	51.4(3)	51.2(1)	51.4(3)	53.4(1)	53.4(3)	54.0(3)
	A	10(2)	11(2)	12(2)	13(2)	10(2)	13(2)
Sextet	IS	0.38(2)	0.36(2)	0.38(2)	0.51(2)	0.56(3)	0.52(2)
component (B)	Heff	48.6(4)	48.9(2)	48.6(4)	51.4(1)	51.5(2)	51.0(3)
	A	6(3)	4(2)	4(3)	16(2)	14(2)	11(2)
Sextet	IS	0.90(2)	0.87(1)	0.92(2)	0.95(2)	1.06(2)	1.06(1)
component (C)	Heff	43.4(2)	46.6(2)	45.1(2)	42.0(3)	43.3(3)	43.8(3)
	A	8(2)	8(2)	9(2)	19(2)	17(2)	15(2)
Sextet	IS	–	–	–	0.61(2)	0.60(2)	0.56(2)
component (D)	Heff	–	–	–	48.9(4)	49.1(2)	47.9(4)
	A	–	–	–	9(3)	11(2)	7(2)

IS: isomer shift, QS: quadruple splitting, Heff: hyperfine field, A: absorption area.

The Mössbauer spectrum parameters are similar for all samples at the same temperature, but the proportion of each species is different. Species of the iron-containing ultrafine particles are almost the same, with their own percentage of different compounds. The spectra at 15 K have an additional component in the magnetic hyperfine splitting sextet, which is not seen in the spectra at room temperature. The main double of the two double components, with IS=0.36 mm/s and QS= 0.68 mm/s at room temperature, converted to a double component with IS=0.42 mm/s and QS= 0.75 mm/s, plus several partly sextet components, hence the significant decrease of the component proportion. This indicates that the iron-containing particles in nano-size show a superparamagnetic behavior at RT but ferromagnetic partly at 15 K. About 29%, 33% and 35% of the micro-, mixed- and nano-sizes were paramag particles. The small size paramag particles may disperse in the water, and may induce oxidative damage to people.

The IS value and QS of the sextet component (A) are close to those of α-Fe_2O_3[23,24], and the three categories of particles have almost the same percentage. The left sextet components are respectively 44%, 42% and 33% in the micro-, mixed- and nano-sized particles, which may be Fe_3O_4 and some sulfate particles. A small fraction of the iron-containing particles shows larger IS and QS values (IS=1.12 mm/s and QS =2.57 mm·s^{-1} at RT, and IS =1.25 mm·s^{-1} and QS = 2.88 mm·s^{-1} at 15 K). We assume that this component, being about 14%, 15% and 18% in the particles outside of tunnel, entrance of tunnel and the middle of tunnel particles, respectively, may be from calcium iron silicate[27,28] or hydrous iron sulfate particle[25]. This indicates that most of the species are not soluble in water, while they have less than 18% soluble fraction. The Mössbauer results indicate that the iron- containing particles having soluble fraction are of a small percentage, and some small-size particles are dispersed in water.

Zinc K-edge XANES spectra and EXAFS spectra of the three kinds of samples are shown in Fig.3. The XANES spectra of the particles collected outside the tunnel and at the entrance are almost the same, but they differ significantly from XANES spectrum of the particles collected inside the tunnel. The zinc may exist as zinc chloride phase in all the samples referring the reference spectra. Based on our researches on single particles of automobile exhaust showing the existence of Cl[15] , we could assume that $ZnCl_2$, which is soluble, is the main speciation in all the particles.

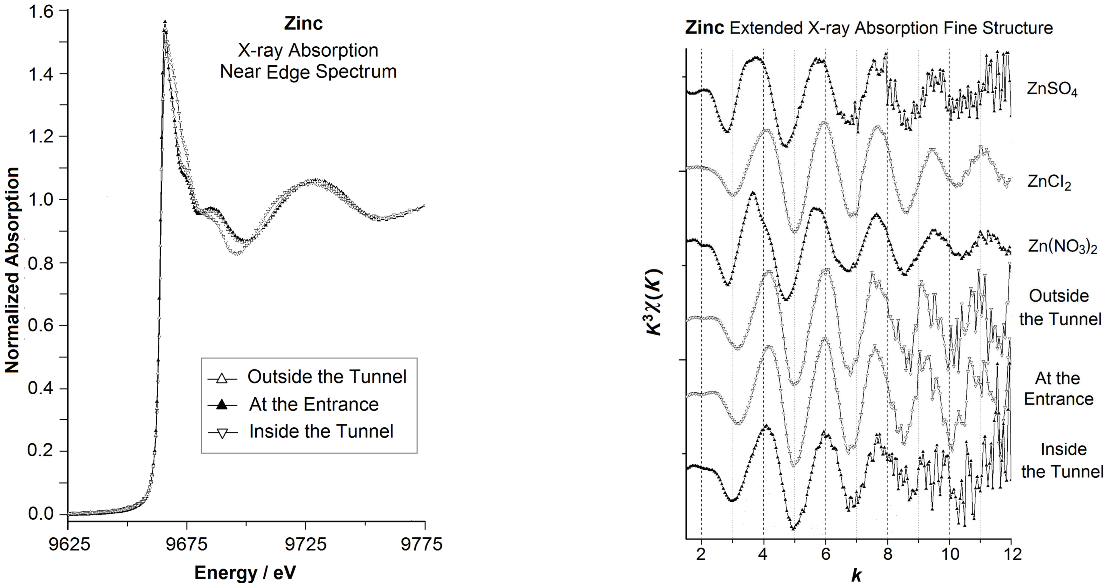

Fig.3 Zn K-edge XANES and EXAFS spectra of the particles collected at the tunnel sites.

The lead L(III)-edge XANES spectra of the samples and reference compound are shown in Fig.4. The pre-edge peak at 13026 eV in PbO_2 is not observed in the sample spectra, hence the absence of PbO_2 in the particles. According to our previous work [27], $PbCl_2$, $PbSO_4$, and PbO were major species in PM_{10} and $PM_{2.5}$ in Shanghai. In addition, $PbSO_4$, $PbCO_3$, PbS, and $Pb_5(PO_4)_3(Cl, OH, F)$ are naturally occurring forms of inorganic lead in the environment [28]. That is why we chose PbSO4, PbS, $Pb_3(PO_4)_2$, PbO, $PbCO_3$, and $PbCl_2$ as the reference compounds. Compared with the reference spectra, none of the particle spectra is similar to any of the reference spectra. This suggests that several lead compounds may co-exist in the lead-containing particles. Principle compound analysis (PCA) shows that $PbSO_4$, $Pb_3(PO_4)_2$, and $PbCO_3$ are main compounds in the particles, with their approximate proportion of 24%, 52%, and 23%, respectively, from the LC-XANES fitting. $PbCO_3$ and $PbSO_4$ are formed from chemical reactions between the oxides of lead, carbon and sulfur at pH=4.93.

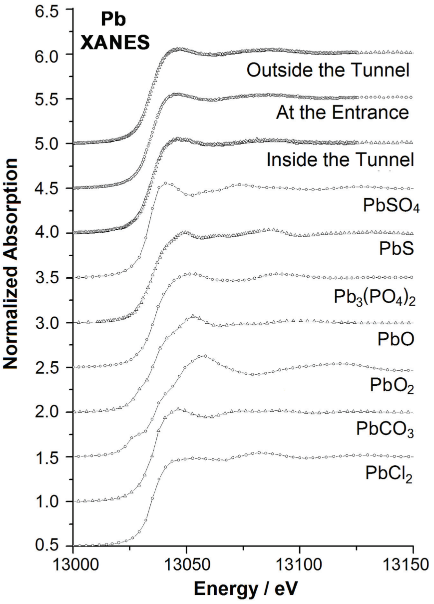

Fig.4 The Pb L(III)-edge spectra of the reference compounds and the particles collected at the tunnel sites.

Studies have shown that oxidative damage to the plasmid DNA is mostly caused by the soluble fraction of the particles[29–32]. We examined the oxidative capacity of soluble fraction of the particles collected outside and in middle of the tunnel by using plasmid DNA assay (Fig.5). The TD20 values (toxic dose causing 20% damage to DNA) of the inside and outside particles were 26.3 and 272.3 µm/mL, respectively. The inside particles had stronger oxidative stress on DNA than that of the outside particles. From the IP-MS and Mössbauer results, the inside particles had higher iron concentration. It is known that iron cation can induce free radicals from H_2O_2 and cause macrophage cytotoxicity and a strong oxidative response[33–36]. Therefore, the stronger damage to the plasmid DNA induced by the micro-sized particles was caused by the particle size and the soluble fraction.

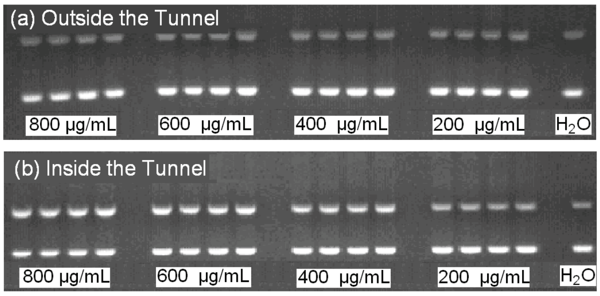

Fig.5 Gel electrophoresis showing oxidative damage to plamid DNA induced by particles from the tunnel sites.

The ICP-MS measurements also showed that the soluble fraction of zinc in particles inside the tunnel (2017 µg/g) was much higher than that the particles inside the tunnel (1042 µg/g). According to Richards[37] and Adamson[38], soluble zinc, rather than insoluble zinc, could cause pulmonary damage and pulmonary cell damage. Therefore, the particles with high concentration of water-soluble zinc compounds had stronger damage to plasmid DNA.

Besides, the concentrations of soluble fraction of Ti, V and Pb in the particles inside the tunnel were much higher than those of the outside particles. These could affect the oxidative damage, too[39,40].

4 Conclusions

Multi-techniques were used to characterize ultrafine particles collected at different positions of the tunnel, and toxicity of the particles was assessed by plasmid DNA. The particles collected in middle of the tunnel are of nanometer size, while the particles collected outside the tunnel are of micro-size. The particles inside the tunnel come mainly from vehicle exhaust. The particles inside the tunnel have higher Fe and Zn concentration than the outside particles, and the main species in the particles is iron oxide or $ZnCl_2$. The soluble fraction of iron and zinc compounds may cause oxidative damage to plasmid DNA.

Acknowledgements

This work was supported by Knowledge Innovation Project of Chinese Academy of Sciences (KJCX3. SYW.N3, key program), and the National Natural Science Foundation of China (10490182, key program; and 10675159). The authors would like to express their thanks to the XAFS station of the Beijing Synchrotron Radiation Facility and XAFS station of the Photon Factory.

Reference

1 Service R F. Sci, 2003, **300:** 243.
2 Brumfiel G. Nat, 2003, **424:** 246–248.
3 Dreher K L. Toxicol Sci, 2004, **77:** 3–5.
4 Service R F. Sci, 2004, **304:** 1732–1734.
5 Auffan M, Rose J, Bottero J Y, *et al.* Nat Nanotechnol, 2009, **4:** 634–641.
6 Belleudi V, Faustini A, Stafoggia M, *et al.* Epidemiol, 2010, **21:** 414–423.
7 Gradon L, Orlicki D, Podgorski A. Int J Occup Saf Ergon, 2000, **6:** 189–207.
8 Oberdorster G, Utell M J. Environ Health Perspect, 2002, **110:** A440–441.
9 Schulz H, Harder V, Ibald-Mulli A, *et al.* J Aerosol Med, 2005, **18:** 1–22.
10 Upadhyay S, Stoeger T, Harder V, *et al.* Part Fibre Toxicol, 2008, **5:** 19.
11 Evans S A, Al-Mosawi A, Adams R A, *et al.* Exp Lung Res, 2006, **32:** 363–378.
12 Jacobsen N R, Moller P, Jensen K A, *et al.* Part Fibre Toxicol, 2009, **6:** 2.
13 Lam C W, James J T, McCluskey R, *et al.* Toxicol Sci, 2004, **77:** 126–134.
14 Nemmar A, Hoet P H, Vanquickenborne B, *et al.* Circulat, 2002, **105:** 411–414.
15 Tong Y, Li A, Cai Y, *et al.* Environ Sci Technol 2001, **35:** 1432–1436.
16 Nomura M. J Synchrotron Radiat, 1998, **5:** 851–853.
17 Nomura M, Koyama A. J Synchrotron Radiat, 1999, **6:** 182–184.
18 Rehr J J, Albers R C, Zabinsky S I. Phys Rev Lett, 1992, **69:** 3397–3400.
19 Troger L, Yokoyama T, Arvanitis D, *et al.* Phys Rev B Condens Matter, 1994, **49:** 888–903.
20 Ressler T. J Synchrotron Radiat 1998, **5:** 118–122.
21 Greenwell L L, Moreno T, Jones T P, *et al.* Free Radic Biol Med 2002, **32:** 898–905.
22 Sioutas C, Delfino R J, Singh M. Environ Health Perspect, 2005, **113:** 947–955.
23 Wertheim G K. Sci, 1964, **144:** 253–259.
24 Kundig W, Bommel H, Constaba G, *et al.* Phys Rev, 1966, **142:** 327–333.
25 Vandenberghe R E, Degrave E, Landuydt C, *et al.* Hyperfine Interact, 1990, **53:** 175–195.
26 Wang C X, Zhu W, Peng A, *et al.* Environ Int, 2001, **26:** 309–313.
27 Tan M G, Zhang G L, Li X L, *et al.* Anal Chem, 2006, **78:** 8044–-8050.
28 Brown G E, Foster A L, Ostergren J D. M P Natl Acad Sci USA, 1999, **96:** 3388–3395.
29 Lu S L, Shao LY, Wu M H, Jiao Z. J Environ Sci, 2006, **18:** 90–95. (in Chinese)
30 Shao L, Shi Z, Jones T P, Li J, *et al.* Sci Total Environ 2006, **367:** 261–272.
31 Jakob R, Roth A, Haas K, *et al.* J Environ Monit, 2010, **12:** 409–416.
32 Cavallo D, Ursini C L, Maiello R, *et al.* Acta Biomed, 2008, **79:** 87–96.
33 Sagripanti J L. Met Ions Biol Syst, 1999, **36:** 179–209.
34 Zastawny TH, Altman S A, Randers-Eichhorn L, *et al.* Free Radic Biol Med 1995, **18:** 1013–1022.
35 Tong Y, Zhang G, Li Y, *et al.* Eur J Radiol, 2006, **58:** 266–272.
36 Kim BY, Han M J, Chung A S. Free Radic Biol Med, 2001, **30:** 686–698.
37 Richards R J, Atkins J, Marrs T C, Brown R F, Masek L. Toxicol, 1989, **54:** 79–88.
38 Adamson I Y, Prieditis H, Hedgecock C, Vincent R. Toxicol Appl Pharmacol, 2000, **166:** 111–119.
39 Wang B, Feng W Y, Wang T C, *et al.* Toxicol Lett, 2006, **161:** 115–123.
40 Jin C, Li Y, Li Y L, *et al.* Nucl Instrum Meth B, 2008, **266:** 3607–3613.